



## Effect of Non-uniform Magnetic Field on Non-newtonian Fluid Separation in a Diffuser

S. M. Moghimi, M. Abbasi\*, M. Khaki Jamei, D. D. Ganji

Department of Mechanical Engineering, Sari Branch, Islamic Azad University, Sari, Iran

### PAPER INFO

#### Paper history:

Received 11 February 2020  
Received in revised form 18 April 2020  
Accepted 11 June 2020

#### Keywords:

Diffuser  
Non-uniform Magnetic Field  
Separation Point  
Second Grade

### ABSTRACT

The purpose of the present study is to investigate the boundary layer separation point in a magnetohydrodynamics diffuser. As an innovation, the  $Re$  value on the separation point is determined for the non-Newtonian fluid flow under the influence of the non-uniform magnetic field due to an electrical solenoid, in an empirical case. The governing equations including continuity and momentum are solved by applying the semi-analytical collocation method (C.M.). The analysis revealed that for specific values of  $De$  from 0.4 to 1.6,  $\alpha$  from  $20^\circ$  to  $2.5^\circ$  and  $Ha$  from zero to 8, the  $Re$  value on the separation point is increased from 52.94 to 1862.78; thus, the boundary layer separation postponed. Furthermore, the impact of the magnetic field intensity on the separation point is analyzed from the physical point of view. It is observed the wall shear stress increases by increasing magnetic field intensity that leads to delaying the boundary layer separation.

doi: 10.5829/ije.2020.33.07a.23

### NOMENCLATURE

$u_{max}$	Inlet velocity (m/s)	$Ha$	Hartmann number
$u_r$	r-component of the velocity (m/s)	<b>Greek Symbols</b>	
$r$	Coordinate in the direction of flow (m)	$\sigma$	Electrical conductivity ( $\Omega.m$ ) <sup>-1</sup>
$P$	Pressure (Pa)	$\alpha$	Diffuser half angle (radian)
$Re$	Reynolds number	$\theta$	Angle between center line and wall (radian)
$t$	Time (s)	$\rho$	Density ( $kg/m^3$ )
$T$	Rivlin Ericksin tensors	$\eta$	Arbitrary variable
$I_0$	Identity tensor	$F(\eta)$	Dimensionless velocity
$R$	Residual	$\alpha_1$	First material constants
$De$	Deborah number	$\alpha_2$	Second material constants
$J$	Density of electric current ( $A/m^2$ )	$\tau$	Shear stress (pa)
$I$	Electric current (A)	$\mu_0$	Permeability of free space (Tm/A)
$B$	Total magnetic field (T)	$\mu_r$	Relative permeability
$B_0$	External magnetic field (T)	$\mu$	Permeability of a specific medium (Tm/A)
$B$	Induced magnetic field (T)	$\mu_f$	Dynamical viscosity (pa.s)
$E$	Electric field (V/m)		

### 1. INTRODUCTION

The interaction of the magnetic field on the electrically conducting fluid flow is called magnetohydrodynamics (MHD). Investigation of the way the magnetic field

affects the boundary layer is an interesting subject for researchers. The study of non-Newtonian fluid flow has been appealing many interests, due to its numerous industrial and engineering applications including polymer technology, condensed matter physics, astrophysics, geophysics, environmental, biophysics and molten plastics, etc. Furthermore, according to

\*Corresponding Author Email: mmortezaabbasi@gmail.com (M. Abbasi)

literature, the subject of the MHD fluid flows have been considered in many research works using different methods [1-5], and fluid flow in the nozzle has been investigated with different methods as well [6, 7]. Makinde [8] investigated the effect of arbitrary magnetic Reynolds number on a steady flow of an incompressible conducting viscous liquid in divergent channels under the influence of an externally applied homogeneous magnetic field. Nourazar et al. [9] studied the MHD flow of non-Newtonian Casson fluid in a stretching/shrinking divergent channel. Their results showed that by increasing the stretching parameter or Reynolds number, due to additional drag force acting on the plate at large values of stretching parameter, the velocity increased. Ara et al. [10] investigated the non-Newtonian fluid flow between the non-parallel walls. It was found that although the angular velocity of micro constituents in the flow increases, the fluid velocity decreases, as the vortex viscosity parameter values augmentation is associated with divergent channel. In addition, the spin gradient viscosity and micro-inertia density both enhance the micro rotation profiles. Umar Khan et al. [11] revealed that Dufour and Soret influence on the second-grade flow in diverging channels with stretchable walls. The results showed that the maximum velocity is obtained in the middle section of the divergent channel. Hayat et al. [12] studied the effects of a second-grade fluid flow in a divergent channel, and showed that the dimensionless velocity is a function of Reynolds number and divergent angle which reduces the velocity. However, when Deborah number increases, the velocity is also increased. The effect of non-uniform magnetic intensity on separation in a diffuser with Newtonian fluid flow is provided by Moghimi et al. [13]. The results indicated that by increasing the magnetic field intensity, the Lorentz force increased; then, the separation point was delayed.

According to the above discussion, although the numerous researches have focused on the MHD and non-Newtonian flows, but the investigation on the flow separation and determination of the separation point for the MHD non-Newtonian flows in a diffuser imposed with the non-uniform magnetic field intensity has not been studied yet. Hence, the aim and novelty of the present study is to compute the separation point for the MHD flows of a second-grade non-Newtonian fluids in divergent channels in the presence of the non-uniform magnetic field for different values of  $Re$ . The semi-analytical collocation method (C.M.) is applied for solving the problem. In addition, the effect of problem parameters on the separation point is presented graphically. Hereafter, the problem will be introduced and governing equations presented. Then, the solution and collocation method will be explained. Thereafter, the results will discussed, and finally, conclusions will be provided.

## 2. PROBLEM STATEMENT

A diffuser with half angle  $\alpha$  subjected to a non-uniform external magnetic field is shown in Figure 1. A laminar, incompressible, steady and second-grade non-Newtonian fluid flows through the diffuser.

The  $r$  and theta ( $\theta$ ) axes are defined as usual polar coordinates. The  $r$ -axis corresponds to the direction of the flow and lies on centerline. The flow velocity distribution is considered. The general governing equations for the defined problem are introduced according to literature [11, 14, 15]:

$$\nabla \cdot \vec{V} = 0 \quad (1)$$

$$\rho \frac{D\vec{V}}{Dt} = -\nabla S + \vec{J} \times \vec{B} \quad (2)$$

$$\vec{J} = \sigma(\vec{E} + \vec{V} \times \vec{B}) \quad (3)$$

$$S = -PI_0 + \tau \quad (4)$$

$$\tau = \mu_f T_1 + \alpha_1 T_2 + \alpha_2 T_1^2 \quad (5)$$

$$T_1 = \nabla V + \nabla V^T \quad (6a)$$

$$T_2 = \frac{D\vec{V}}{Dt} + T_1 \nabla V + \nabla V^T T_1 \quad (6b)$$

Equations (1) to (3) are continuity, momentum and Ohm's law, respectively.  $\vec{V}$ ,  $\vec{J}$ ,  $E$ ,  $\sigma$ ,  $I_0$ ,  $\mu_f$ ,  $\tau$ ,  $T_1$ ,  $T_2$ ,  $\nabla$ ,  $\alpha_1$  and  $\alpha_2$  are the velocity vector, the electric current density, the electric field intensity, electrical conductivity, the pressure, identity tensor, the dynamic viscosity, the shear stress, first and second Rivlin Ericksin tensors, Laplacian operator and material constants, respectively [11, 16]. The total magnetic field is  $B = B_0 + b$ , where  $B_0$  and  $b$  are the external and induced

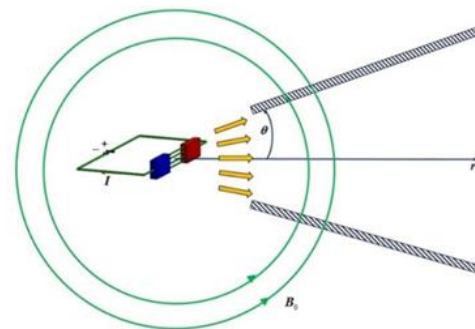


**Figure 1.** Schematic of a diffuser under the influence of a non-uniform magnetic field

magnetic fields, respectively. In the problem at hand, the magnetic Reynolds number is assumed small enough, so that the induced magnetic field can be neglected [15].

The cell electric current enters a solenoid, including parallel wires, by a distributor. The wires current is collected by a collector and returned back to the cell. Due to the electrical current in solenoid wires, a magnetic field is generated around the solenoid with intensity proportional to the distance from solenoid center, as shown in Figure 1. The applied magnetic field ( $B_0$ ) can be obtained as:

$$B_0 = \frac{\mu I}{2 \pi r}, \quad \mu = \mu_0 \cdot \mu_r \tag{7}$$

where  $\mu$ ,  $\mu_r$  and  $\mu_0$  are the specific medium permeability, the relative permeability, and the permeability of the free space, respectively.  $\mu_0$  is constant and equal to  $4\pi \times 10^{-7}$  (Tm/A),  $r$  the distance from the center of solenoid and  $I$  the electric current. According to Equation (7), the magnetic field intensity is a function of the radius and current, thus, it can be regulated by changing the electrical current magnitude.

From Equations (1) and (2), the continuity and momentum equations in  $r$  and  $\theta$  direction are given as [11, 16]:

$$\frac{1}{r} \frac{\partial r u_r}{\partial r} = 0 \tag{8a}$$

$$u_r \frac{\partial u_r}{\partial r} = -\frac{\partial P}{\rho \partial r} + \frac{\mu_r}{\rho} \left( 2 \frac{\partial^2 u_r}{\partial r^2} + \frac{2}{r} \frac{\partial u_r}{\partial r} + \frac{1}{r^2} \frac{\partial^2 u_r}{\partial \theta^2} - \frac{2u_r}{r^2} \right) - \frac{\alpha_1}{\rho} \left( \frac{2u_r}{r} \frac{\partial^2 u_r}{\partial r^2} + 2 \frac{\partial u_r}{\partial r} \frac{\partial^2 u_r}{\partial r^2} - \frac{1}{r^3} (\frac{\partial u_r}{\partial \theta})^2 + 2u_r \frac{\partial^3 u_r}{\partial r^3} - \frac{1}{r^2} \frac{\partial u_r}{\partial r} \frac{\partial^2 u_r}{\partial r \partial \theta} \right) - \frac{\alpha_1}{\rho} \left( \frac{1}{r^2} \frac{\partial^2 u_r}{\partial r \partial \theta} + \frac{\partial u_r}{\partial r} \frac{\partial^2 u_r}{\partial \theta^2} - \frac{2u_r}{r^3} \frac{\partial^2 u_r}{\partial \theta^2} - \frac{u_r}{r^2} \frac{\partial^3 u_r}{\partial r^2 \partial \theta} + 2 \frac{u_r^3}{r^3} - \frac{2u_r}{r^2} \frac{\partial u_r}{\partial r} \right) - \frac{\sigma}{\rho} u_r B_0^2 \tag{8b}$$

$$u_r \frac{\partial u_r}{\partial r} = -\frac{\partial P}{\rho \partial r} + \frac{\mu_r}{\rho} \left( 2 \frac{\partial^2 u_r}{\partial r^2} + \frac{2}{r} \frac{\partial u_r}{\partial r} + \frac{1}{r^2} \frac{\partial^2 u_r}{\partial \theta^2} - \frac{2u_r}{r^2} \right) - \frac{\alpha_1}{\rho} \left( \frac{2u_r}{r} \frac{\partial^2 u_r}{\partial r^2} + 2 \frac{\partial u_r}{\partial r} \frac{\partial^2 u_r}{\partial r^2} - \frac{1}{r^3} (\frac{\partial u_r}{\partial \theta})^2 + 2u_r \frac{\partial^3 u_r}{\partial r^3} - \frac{1}{r^2} \frac{\partial u_r}{\partial r} \frac{\partial^2 u_r}{\partial r \partial \theta} \right) - \frac{\alpha_1}{\rho} \left( \frac{1}{r^2} \frac{\partial^2 u_r}{\partial r \partial \theta} + \frac{\partial u_r}{\partial r} \frac{\partial^2 u_r}{\partial \theta^2} - \frac{2u_r}{r^3} \frac{\partial^2 u_r}{\partial \theta^2} - \frac{u_r}{r^2} \frac{\partial^3 u_r}{\partial r^2 \partial \theta} + 2 \frac{u_r^3}{r^3} - \frac{2u_r}{r^2} \frac{\partial u_r}{\partial r} \right) - \frac{\sigma}{\rho} u_r B_0^2 \tag{8c}$$

where  $u_r$  is a radial velocity in direction of flow through diffuser, and  $\mu_r$  is the dynamic viscosity. The boundary conditions are defined as follows:

$$\theta = 0: \quad u_r = u_{\max} \tag{9a}$$

$$\theta = 0: \quad \frac{\partial u_r}{\partial \theta} = 0 \tag{9b}$$

$$\theta = \alpha, -\alpha: \quad u_r = 0 \tag{9c}$$

Integrating Equation (8a) and using Equation (9b) gives:

$$u_r = \frac{1}{r} f(\theta) \tag{10}$$

To eliminate pressure gradient, Equations (8b) and (8c) are differentiated with respect to  $\theta$  and  $r$ , respectively, and then subtracting from each other. Afterwards, by employing the similarity dimensionless variables as [17]:

$$\eta = \frac{\theta}{\alpha} \tag{11a}$$

$$F(\eta) = \frac{u_r}{u_{\max}} = \frac{1}{r} \frac{f(\theta)}{u_{\max}} \tag{11b}$$

In addition, after some simplifications, the governing equations reduces to:

$$F'' + 2\alpha \text{Re} F F' + (4\alpha^2 - \text{Ha}^2) F' + 4\text{De} (F F'' + 4\alpha^2 F F') = 0 \tag{12a}$$

$$\text{Re} = \frac{u_{\max} r \alpha}{\nu} \tag{12b}$$

$$\text{Ha} = B_0 r \alpha \sqrt{\frac{\sigma}{\mu_r}} \tag{12c}$$

$$\text{De} = -\frac{\alpha_1 u_{\max}}{r \mu_r} \tag{12d}$$

Here,  $\text{Re}$  denotes the Reynolds number,  $\text{Ha}$  is the Hartmann number and  $\text{De}$  represents Deborah number which are dimensionless physical quantities. In the present investigation, the skin friction coefficient is the intended physical quantity which is calculated as [12]:

$$C_f = \frac{1}{\text{Re}} F'(\eta) \tag{13}$$

The  $\text{Re}$  value pertinent to separation is shown with  $\text{Re}_{\text{Sep}}$ . It happens when  $C_f$  becomes zero. On the other hand, according to Equation (13), when  $F'(\eta) = 0$  the separation occurs.

Furthermore, the boundary conditions are

transformed into the dimensionless form as follows:

$$\eta = 0: \quad F(0) = 1 \quad (14a)$$

$$\eta = 1: \quad F(1) = 0 \quad (14b)$$

$$\eta = 0: \quad F'(0) = 0 \quad (14c)$$

## 2. 1. The Problem Solution

Two different methods are conducted to solve for the current problem. In the first method, the numerical method is employed to achieve dimensionless velocity distribution data. By using trial and error, the Re value related to  $F'(1) = 0$  for different values of Ha, De and  $\alpha$  is obtained and called  $Re_{Sep}$ .

In the other method, the Collocation Method (C.M.) [17-19], described in the following section, is used to obtain the dimensionless velocity distribution relation. The velocity distribution is plotted using the obtain relation. It is expected to see a reverse flow to occur for some Re values greater than  $Re_{Sep}$ .

### 2. 1. 1. Collocation Method

The semi-analytical collocation method is used for solving the governing equation. In this method, a trial function is approximated which satisfies the boundary conditions. By inserting the approximated trial function into the governing equations, it is expected that the residuals to be zero. However, due to the approximate solution, the residual does not exactly equal to zero, but it approaches zero. Obviously, as much as the residual value becomes closer to zero, the approximated function has more accuracy.

In this investigation, a polynomial trial function is applied to approximate the solution as follows:

$$F(\eta) = c_{18}\eta^{18} + c_{17}\eta^{17} + c_{16}\eta^{16} + c_{15}\eta^{15} + c_{14}\eta^{14} + c_{13}\eta^{13} + c_{12}\eta^{12} + c_{11}\eta^{11} + c_{10}\eta^{10} + c_9\eta^9 + c_8\eta^8 + c_7\eta^7 + c_6\eta^6 + c_5\eta^5 + c_4\eta^4 + c_3\eta^3 + c_2\eta^2 + c_1\eta^1 + c_0 \quad (15)$$

Equation (15) has 19 unknown coefficients which have to be determined. First, in order that Equation (15) satisfied the boundary conditions described in Equation (14), the boundary conditions are inserted in Equation (15) which yields:

$$c_0 = 1 \quad (16a)$$

$$c_1 = 0 \quad (16b)$$

$$1 + c_2 + c_3 + c_4 + \dots = 0 \quad (16c)$$

Thus, Equation (15) can be rewritten as:

$$F(\eta) = c_{18}\eta^{18} + c_{17}\eta^{17} + c_{16}\eta^{16} + c_{15}\eta^{15} + c_{14}\eta^{14} + c_{13}\eta^{13} + c_{12}\eta^{12} + c_{11}\eta^{11} + c_{10}\eta^{10} + c_9\eta^9 + c_8\eta^8 + c_7\eta^7 + c_6\eta^6 + c_5\eta^5 + c_4\eta^4 + c_3\eta^3 + c_2\eta^2 + 1 \quad (17)$$

Therefore, Equation (17) is the approximated trial function which satisfied the problem boundary conditions. As can be seen in Equation (17), there is 16 unknown coefficients. Hence, 16 equations are required for determining the coefficient. For determining the unknown coefficient, the following procedure is conducted using the collocation method. First, Equation (17) is replaced in Equation (12a) for the case of  $Re=350$ ,  $De=0.8$ ,  $Ha=4$  and  $\alpha = 5^\circ$ , which gives:

$$R(c_2, c_3, \dots, c_{18}, \eta) = 6c_3 + 24c_4\eta + 60c_5\eta^2 + 120c_6\eta^3 + 210c_7\eta^4 + 336c_8\eta^5 + \dots + 4896c_{18}\eta^{15} + 2\alpha Re (2c_2\eta^1 + 3c_3\eta^2 + \dots + 18c_{18}\eta^{17})(1 + c_2\eta^2 + c_3\eta^3 + \dots + c_{18}\eta^{18}) + (4\alpha^2 - Ha^2)(2c_2\eta^1 + 3c_3\eta^2 + \dots + 17c_{17}\eta^{16} + 18c_{18}\eta^{17}) + 4De[(1 + c_2\eta^2 + c_3\eta^3 + \dots + c_{18}\eta^{18})(6c_3 + 24c_4\eta + \dots + 4896c_{18}\eta^{15}) + 4\alpha^2(2c_2\eta^1 + 3c_3\eta^2 + \dots + 18c_{18}\eta^{17})(1 + c_2\eta^2 + c_3\eta^3 + \dots + c_{18}\eta^{18})] \quad (18)$$

It is known that  $\eta$  domain is between zero and one ( $0 < \eta < 1$ ). In the collocation method, the domain is divided into finite intervals the values of which depends on the number of the trial function for unknown coefficients. Therefore, the domain is divided into 16 intervals as the residual become zero:

$$R\left(\frac{1}{17}\right) = 0, R\left(\frac{2}{17}\right) = 0, \dots, R\left(\frac{16}{17}\right) = 0 \quad (19)$$

By inserting each value of the interval in Equation (18), 16 equations are obtained. By solving the set of equations, the unknown coefficients are computed and the approximated trial function is calculated as:

$$F(\eta) = -2.567900139\eta^{18} + 16.03918792\eta^{17} - 41.62834552\eta^{16} + 52.06904837\eta^{15} - 11.88853492\eta^{14} - 68.20484287\eta^{13} + 130.2747688\eta^{12} - 133.8834906\eta^{11} + 93.23789869\eta^{10} - 47.17891722\eta^9 + 18.12684323\eta^8 - 4.992575696\eta^7 - 0.04929084927\eta^6 - 0.16058893\eta^5 + 1.844560443\eta^4 - 0.0012939369\eta^3 - 2.036526779\eta^2 + 1 \quad (20)$$

Here,  $F(\eta)$  is the dimensionless velocity distribution, according to Equation (10b).

**2. 1. 1. Numerical Method** In order to validate the results of the collocation method, the numerical 4th order Runge-Kutta method [20] is used to solve Equation (12a). Thus, Equation (12a) is rewritten as:

$$F''(\eta) = -\frac{A_1 F(\eta) F'(\eta) + A_2 F'(\eta)}{(1 + A_3 F(\eta))} \tag{21}$$

where  $A_1$ ,  $A_2$  and  $A_3$  are constant values equal to  $(2\alpha Re + 16\alpha^2 De)$ ,  $(4\alpha^2 - Ha^2)$  and  $(4De)$ , respectively. Now, to solve Equation (12a) by numerical method, it can be rewritten as a set of equations:

$$F'(\eta) = G(\eta), F(0) = 1 \tag{22a}$$

$$G'(\eta) = H(\eta), G(0) = 0 \tag{22b}$$

$$H'(\eta) = -\frac{A_1 F(\eta) G(\eta) + A_2 G(\eta)}{(1 + A_3 F(\eta))}, H(0) = ? \tag{22c}$$

To solve the above set of equations, three initial values of  $F(0)$ ,  $G(0)$  and  $H(0)$  are required which  $H(0)$  is not determined. Thus, we assume a value for  $H(0)$  and then solve using the shooting method as far as the boundary condition  $F(1)=0$  is satisfied. Now, the set of equations (22) is solved using the 4<sup>th</sup> order Runge-Kutta method.

No reference in literature exactly coincides with the defined problem (especially the non-uniform magnetic intensity); hence, for validation, the results from two methods will be compared. Besides, in Figure 2, for verification, the results for a special case ( $Ha=0$ ,  $De=0.8$ ,  $Re=40$ , and  $\alpha=5^\circ$ ) is plotted and compared with the that of Ref. [12]. It can be seen that there is good agreement between the two. The results for the dimensionless velocity obtained from the two different solutions, i.e. the numerical method and C.M., are presented in Table 1. The comparison of the results shows the reasonable agreement between them.

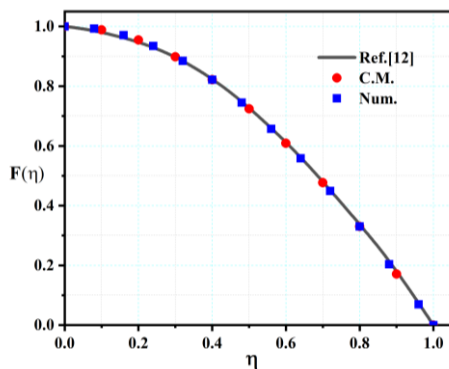


**Figure 2.** Comparison of the present study result with Ref. [12] result

**TABLE 1.** The dimensionless velocity distribution  $F(\eta)$  comparison for C.M. and numerical method at  $Ha=4$ ,  $De=0.8$ ,  $Re_{sep}=568.31$  and  $\alpha=5^\circ$

$\eta$	<b>Re=350</b>		
	<b>C.M.</b>	<b>Numerical</b>	<b>Diff.</b>
0.0	1.0000	1.0000	0.0000
0.1	0.9798	0.9798	0.0000
0.2	0.9213	0.9214	0.0001
0.3	0.8307	0.8307	0.0000
0.4	0.7166	0.7167	0.0001
0.5	0.5893	0.5894	0.0001
0.6	0.4585	0.4585	0.0000
0.7	0.3318	0.3318	0.0000
0.8	0.2139	0.2138	0.0001
0.9	0.1048	0.1048	0.0000
1.0	0.0000	0.0000	0.0000
$\eta$	<b>Re=450</b>		
	<b>C.M.</b>	<b>Numerical</b>	<b>Diff.</b>
0.0	1.0000	1.0000	0.0000
0.1	0.9731	0.9731	0.0000
0.2	0.8963	0.8963	0.0000
0.3	0.7805	0.7806	0.0001
0.4	0.6411	0.6410	0.0001
0.5	0.4948	0.4949	0.0001
0.6	0.3563	0.3563	0.0000
0.7	0.2355	0.2355	0.0000
0.8	0.1371	0.1371	0.0000
0.9	0.0601	0.0601	0.0000
1.0	0.0000	0.0000	0.0000
$\eta$	<b>Re=568.31</b>		
	<b>C.M.</b>	<b>Numerical</b>	<b>Diff.</b>
0.0	1.0000	1.0000	0.0000
0.1	0.9635	0.9635	0.0000
0.2	0.8611	0.8612	0.0001
0.3	0.7118	0.7119	0.0001
0.4	0.5414	0.5414	0.0000
0.5	0.3754	0.3755	0.0001
0.6	0.2334	0.2335	0.0001
0.7	0.1255	0.1256	0.0001
0.8	0.0532	0.0532	0.0000
0.9	0.0126	0.0128	0.0002
1.0	0.0000	0.0000	0.0000
$\eta$	<b>Re=650</b>		
	<b>C.M.</b>	<b>Numerical</b>	<b>Diff.</b>
0.0	1.0000	1.0000	0.0000
0.1	0.9562	0.9562	0.0000

0.2	0.8348	0.8348	0.0000
0.3	0.6618	0.6618	0.0000
0.4	0.4715	0.4715	0.0000
0.5	0.2958	0.2957	0.0001
0.6	0.1557	0.1557	0.0000
0.7	0.0595	0.0594	0.0001
0.8	0.0047	0.0047	0.0000
0.9	-0.0139	-0.0140	0.0001
1.0	0.0000	0.0000	0.0000

$\alpha=10^\circ$				
0	110.09	158.77	206.25	253.08
1	117.06	166.13	213.88	260.91
2	138.29	188.49	237.03	284.66
3	174.77	226.76	276.52	325.09
4	228.26	282.57	333.90	383.65
5	301.33	358.46	411.55	462.57
6	396.90	457.75	512.86	565.14
7	517.19	583.83	641.77	695.54
8	662.65	738.69	801.60	857.99

$\alpha=20^\circ$				
0	52.94	76.37	99.22	121.76
1	56.41	80.04	103.03	125.67
2	67.00	91.19	114.58	137.52
3	85.19	110.28	134.28	157.70
4	111.86	138.12	162.91	186.91
5	148.29	175.97	201.64	226.29
6	195.97	225.49	252.17	277.46
7	256.02	288.41	316.49	342.52
8	328.68	365.73	396.28	423.59

**2. 2. Results and Discussion** In Tables 2a-2d, the results from C.M. are presented. It can be seen that as Ha increases while De and  $\alpha$  decrease, the value of Re, in which the separation occurs, increases. For example, in Table 2b, when the Ha increases from zero to 4 (at De=0.8 and  $\alpha=5^\circ$ ), the value of Re<sub>Sep</sub> is increased about 77.2%, and the De increases from 0.4 to 1.6 (at Ha=4 and  $\alpha=5^\circ$ ), the value of Re<sub>Sep</sub> is increased about 62.4%. In Table 2a-2d  $\alpha$  decreases from 20° to 2.5° at Ha=4 and De=0.8, the value of Re<sub>Sep</sub> is increased about 72.4%. It should be noted that the Re values smaller than Re<sub>Sep</sub> (for the specified problem), the separation does not occur.

**TABLE 2.** The Re<sub>Sep</sub> values for some Ha, and De at the separation point ( F'(1) = 0 ) for different angle of diffuser

$\alpha=2.5^\circ$				
De \ Ha	0.4	0.8	1.2	1.6
0	445.65	642.65	834.79	1024.27
1	473.56	672.11	865.32	1055.62
2	558.55	761.61	957.96	1150.67
3	704.58	914.78	1116.06	1312.52
4	918.74	1138.2	1345.74	1546.88
5	1211.27	1442.0	1656.59	1862.78
6	1593.83	1839.4	-	-

$\alpha=5^\circ$				
0	222.30	320.57	416.41	510.94
1	236.25	335.29	431.68	526.61
2	278.73	380.04	477.99	574.13
3	351.74	456.61	557.03	655.04
4	458.80	568.31	671.85	772.20
5	605.04	720.19	827.25	930.14
6	796.29	918.89	1029.97	1135.39
7	1036.9	1171.17	1287.93	1396.34
8	1327.9	1480.98	1607.72	1721.39

Figure 3 demonstrates the variation of Re<sub>Sep</sub> with respect to Ha for different De values at four channel divergent angles. The second-grade fluid definition,  $\mu_f$ , which is the first viscosity coefficient (the dynamic viscosity), has higher weight than the second viscosity coefficient  $\alpha_1$ . With increasing  $\mu_f$  while De decreases, the momentum near the wall decreases more rapidly, leads to the earlier separation.

The influence of different dimensionless quantities, the Re, De, Ha, and  $\alpha$  are shown in Figures 4 and 5.

As seen in Equation (12), the skin friction coefficient (the wall shear stress) is proportional to F'(η). The effect of Re on F(η) and F'(η) are shown in Figures 4a and 5a, respectively. As shown in Table 2b, the separation Reynolds number value is 568.31. Therefore, as the Reynolds number reaches this value, F(η) is getting tangent to the wall, while on the contrary, F'(η) value becomes zero on the wall. When the Reynolds number continues to increase, the reverse flow develops.

Figures 4b and 5b show variations of F(η) and F'(η) versus De. These figures are for Re=568.31, Ha=4 and  $\alpha = 5^\circ$ .

According to Table 2b, the separation occurs at De=0.8. With increasing De, the shear stress at the wall increases and the momentum along the flow decreases

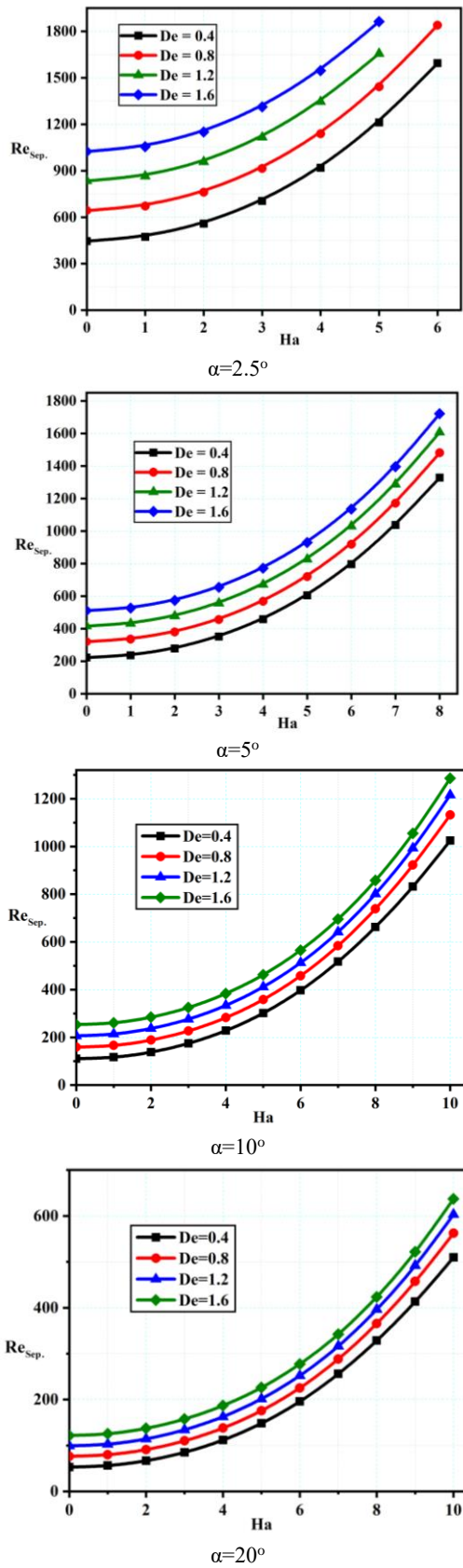


Figure 3. The effect of Ha and De on separation point for different angle of diffuser

and approaches zero. As shown in Figure 4b, the flow over the wall gets tangent and according to Figure 5b, becomes zero. Proceeding along the wall, the reverse flow develops.

The effect of Hartman number on  $F(\eta)$  and  $F'(\eta)$  are shown in Figures 4c and 5c, for  $De=0.8$ ,  $Re=568.31$  and  $\alpha = 5^\circ$ . According to Table 2b, the separation occurs at  $Ha=4$  and the reverse flow is observed for  $Ha$  less than 4. As shown in Figure 4c, for  $Ha=4$  the flow velocity is tangent to the wall, and according to Figure 5c, the value of  $F'(1)$  is zero. With increasing  $Ha$ , i.e. magnetic field intensity augmentation, the momentum near the wall increases such that the separation will not occur. As can be seen, the reverse flow will not happen. In physical aspect, the magnetic Lorentz force is proportional to the velocity and its value in the centerline region is more than in the wall region. Thus, for a special mass flow value, when the magnetic field intensity increases, the momentum near the wall increases, which leads to the separation.

It is expected that with increasing the channel divergent angle, the separation is expedited. This phenomenon can be observed in Figures 4d and 5d. According to Table 2c, for  $Ha=4$ ,  $Re=282.57$  and  $De=0.8$ , the separation happens at  $\alpha = 10^\circ$ . With increasing the channel divergent angel, the reverse flow occurs.

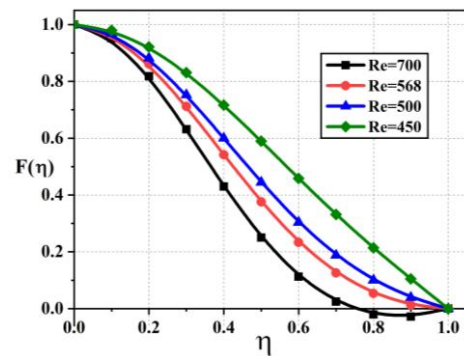


Figure 4a. The Re effect on  $F(\eta)$  for  $De=0.8$ ,  $Ha=4$  and  $\alpha=5^\circ$

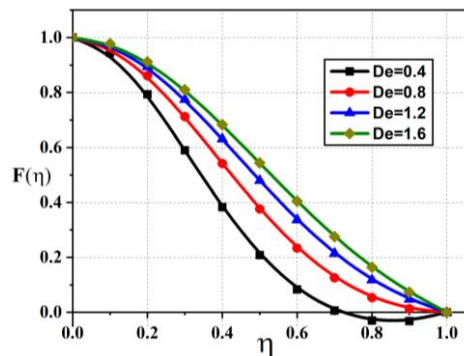
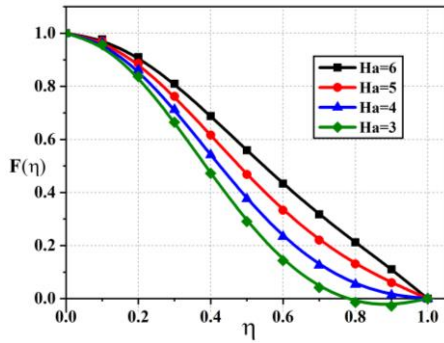
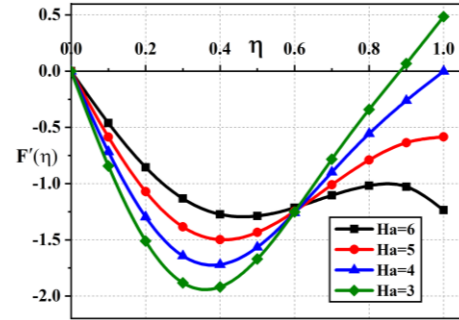


Figure 4b. Debora number effect on  $F(\eta)$  for  $Re=568.31$ ,  $Ha=4$  and  $\alpha=5^\circ$



**Figure 4c.** Hartmann number effect  $F(\eta)$  for  $Re=568.31$ ,  $De=0.8$  and  $\alpha=5^\circ$



**Figure 5c.** Hartmann number effect  $F'(\eta)$  for  $Re=568.31$ ,  $De=0.8$  and  $\alpha=5^\circ$

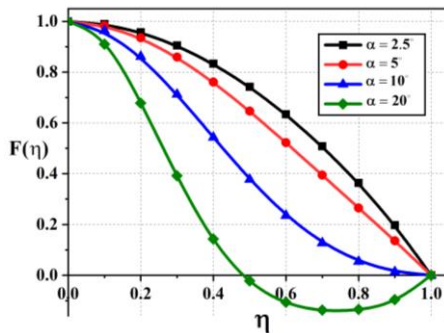


**Figure 4d.** Half divergent angle effect on  $F(\eta)$  for  $Re=282.57$ ,  $De=0.8$  and  $Ha=4$

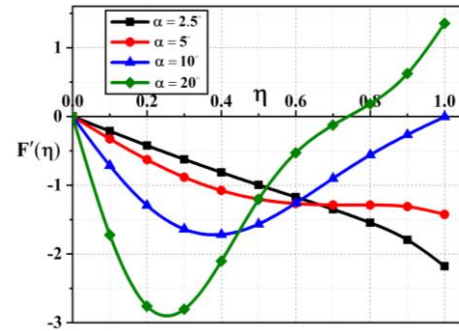


**Figure 5d.** Half divergent angle effect on  $F'(\eta)$  for  $Re=282.57$ ,  $De=0.8$  and  $Ha=4$

Figure 6 shows the  $C_f$  values versus  $Re$  for  $De=0.8$  at different values of  $Ha$ . Where the  $C_f$  value becomes

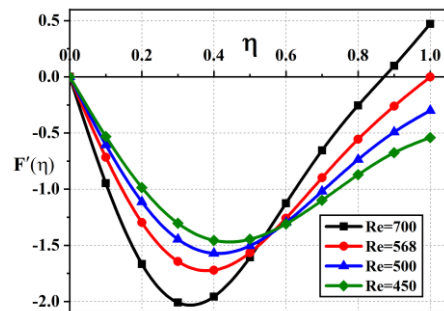


**Figure 5a.** The  $Re$  effect on  $F'(\eta)$  for  $De=0.8$ ,  $Ha=4$  and  $\alpha=5^\circ$

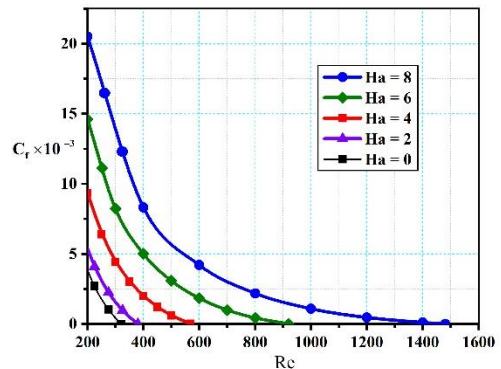


**Figure 6.** The  $Ha$  effect on Friction Factor  $C_f$  for  $De=0.8$  and  $\alpha=5^\circ$

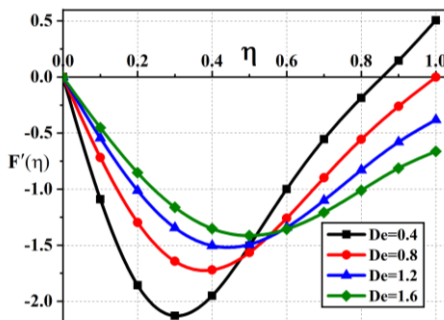


**Figure 5b.** Debora number effect on  $F'(\eta)$  for  $Re=568.31$ ,  $Ha=4$  and  $\alpha=5^\circ$

zero, the  $Re$  value corresponds to the one for separation. The effect of  $Ha$  augmentation in this case is similar for Figures 4c and 5c, as discussed earlier.

### 3. CONCLUSIONS

In this article, the separation point of a non-Newtonian second-grade fluid flow through a diffuser was investigated. The imposed magnetic field intensity and viscous fluid degree effects on the flow were studied. As an innovation, for non-Newtonian fluid flow, the  $Re$  value on the separation point is determined under the influence of the non-uniform magnetic field due to an

electrical solenoid, at an empirical case. The effect of material parameter of second-grade fluid and magnetic field intensity on the skin friction coefficient is opposite and by increasing of the magnetic field intensity ( $Ha$ ), the Lorentz force increases which leads to delay in the separation. It was observed when  $\alpha=5^\circ$  and  $Ha$  changes from 0 to 8, for  $De=0.4$ ,  $Re_{sep}$  increases 498%, for  $De=0.8$ ,  $Re_{sep}$  increases 362%, for  $De=1.2$ ,  $Re_{sep}$  increases 286% and for  $De=1.6$ ,  $Re_{sep}$  increases 231%. This augmentation was also observed for other values of  $\alpha$ . Moreover, in a diffuser with certain conditions, by adjustable magnetic field intensity, one can increase the magnitude of the Lorentz force up to a level that the separation does not occur on the walls. Furthermore, the analysis indicated that the dimensionless velocity distribution becomes flatter when  $Ha$ ,  $De$  and  $\alpha$  increases. Besides the effects of  $Re$ ,  $De$  and  $Ha$  on the skin friction coefficient  $C_f$  was presented.

#### 4. REFERENCES

1. Cruze, D., Hemalatha, G., Jebadurai, S.V.S., Sarala, L., Tensing, D., and Christy, S.J.E., "A review on the magnetorheological fluid, damper and its applications for seismic mitigation", *Civil Engineering Journal*, Vol.4, No. 12, (2018), 3058-3074. DOI: 10.28991/cej-03091220
2. Dirbude, S.B., and Maurya, V.K., "Effect of Uniform Magnetic Field on Melting at Various Rayleigh Numbers", *Emerging Science Journal*, Vol. 3, No. 4, (2019), 263-273. DOI: 10.28991/esj-2019-01189
3. Ghadikolaie, S., Hosseinzadeh, K., and Ganji, D., "Analysis of unsteady MHD Eyring-Powell squeezing flow in stretching channel with considering thermal radiation and Joule heating effect using AGM", *Case studies in thermal engineering*, Vol. 10, (2017), 579-594. DOI: 10.1016/j.csite.2017.11.004
4. Sears, F.W., Zemansky, M.W., Young, H.D., and Freedman, R.A., "Sears and Zemansky's University Physics: With Modern Physics", Addison-Wesley, New York, (2012). ISBN: 0321696867, 9780321696861
5. Taheri, M.H., Abbasi, M., and Jamei, M.K., "An integral method for the boundary layer of MHD non-Newtonian power-law fluid in the entrance region of channels", *Journal of the Brazilian Society of Mechanical Sciences and Engineering*, Vol. 39, No. 10, (2017), 4177-4189. DOI: 10.1007/s40430-017-0887-5
6. Sengupta, A.R., Gupta, R., and Biswas, A., "Computational Fluid Dynamics Analysis of Stove Systems for Cooking and Drying of Muga Silk", *Emerging Science Journal*, Vol. 3, No. 5, (2019), 285-292. DOI: 10.28991/esj-2019-01191
7. Su, C., and Cheng, Y.-h., "Numerical and Experimental Research on Convergence Angle of Wet Sprayer Nozzle", *Civil Engineering Journal*, Vol. 4, No. 9, (2018), 1985-1995. DOI: 10.28991/cej-03091132
8. Makinde, O., "Effect of arbitrary magnetic Reynolds number on MHD flows in convergent-divergent channels", *International Journal of Numerical Methods for Heat & Fluid Flow*, Vol. 18, No. 6, (2008), 697-707. DOI:10.1108/09615530810885524
9. Nourazar, S., Nazari-Golshan, A., and Soleymannpour, F., "On the expedient solution of the magneto-hydrodynamic Jeffery-Hamel flow of Casson fluid", *Scientific reports*, Vol. 8, No. 1, (2018), 1-16. DOI: 10.1038/s41598-018-34778-w
10. Ara, A., Khan, N.A., Naz, F., Raja, M.A.Z., and Rubbab, Q., "Numerical simulation for Jeffery-Hamel flow and heat transfer of micropolar fluid based on differential evolution algorithm", *AIP Advances*, Vol. 8, No. 1, (2018), 1-17. DOI: 10.1063/1.5011727
11. Khan, U., Ahmed, N., and Mohyud-Din, S.T., "Soret and Dufour effects on Jeffery-Hamel flow of second-grade fluid between convergent/divergent channel with stretchable walls", *Results in physics*, Vol. 7, (2017), 361-372. DOI: 10.1016/j.rinp.2016.12.020
12. Hayat, T., Nawaz, M., and Sajid, M., "Effect of heat transfer on the flow of a second-grade fluid in divergent/convergent channel", *International Journal for Numerical Methods in Fluids*, Vol. 64, No. 7, (2010), 761-776. DOI: 10.1002/fld.2170
13. Moghimi, S.M., Abbasi, M., Jamei, M.K., and Ganji, D.D., "Boundary-layer separation in circular diffuser flows in the presence of an external non-uniform magnetic field", *Mechanical Sciences*, Vol. 11, No. 1, (2020), 39-48. DOI: 10.5194/ms-11-39-2020
14. Christov, I.C., "Stokes' first problem for some non-Newtonian fluids: Results and mistakes", *Mechanics Research Communications*, Vol. 37, No. 8, (2010), 717-723. DOI:10.1016/j.mechrescom.2010.09.006
15. Roidt, M., and Cess, R., "An approximate analysis of laminar magneto-hydrodynamic flow in the entrance region of a flat duct", *Journal of Applied Mechanics*, Vol. 29, No. 1, (1962), 171-176. DOI: 10.1115/1.3636451
16. Khan, U., Ahmed, N., and Mohyud-Din, S.T., "Thermo-diffusion and diffusion-thermo effects on flow of second grade fluid between two inclined plane walls", *Journal of Molecular Liquids*, Vol. 224, (2016), 1074-1082. DOI: 10.1016/j.molliq.2016.10.068
17. Kazemi, K.B., "Solving differential equations with least square and collocation methods", Master thesis, George Washington University, USA, (2004).
18. Ebrahimi, S., Abbasi, M., and Khaki, M., "Fully developed flow of third-grade fluid in the plane duct with convection on the walls", *Iranian Journal of Science and Technology, Transactions of Mechanical Engineering*, Vol. 40, No. 4, (2016), 315-324. DOI: 10.1007/s40997-016-0031-7
19. Gavabari, R.H., Abbasi, M., Ganji, D., Rahimpetroudi, I., and Bozorgi, A., "Application of Galerkin and Collocation method to the electrohydrodynamic flow analysis in a circular cylindrical conduit", *Journal of the Brazilian Society of Mechanical Sciences and Engineering*, Vol. 38, No. 8, (2016), 2327-2332. DOI: 10.1007/s40430-014-0283-3
20. Hussain, K., Ismail, F. and Senu, N., "Runge-Kutta Type Methods for Directly Solving Special Fourth-Order Ordinary Differential Equations", *Mathematical Problem Engineering*, Vol. 2015, (2015), 1-11. DOI: 10.1155/2015/893763

---

**Persian Abstract**

---

**چکیده**

هدف از این مطالعه، بررسی نقطه‌ی جدایش لایه‌ی مرزی برای جریان هیدرودینامیک مغناطیسی در یک دیفیوزر است. به عنوان نوآوری، برای جریان سیال غیرنیوتونی تحت تأثیر میدان مغناطیسی نایک‌نواخت که توسط یک سلونوئید الکتریکی ایجاد شده، مقدار عدد رینولدز در نقطه‌ی جدایش تعیین می‌شود. معادلات حاکم شامل معادلات پیوستگی و ممنتوم با استفاده از روش نیمه‌تحلیلی تلفیقی حل می‌شوند. تحلیل نتایج نشان می‌دهد که برای مقادیر ویژه هنگامی که عدد دیوار از  $0/4$  تا  $1/6$ ، نصف زاویه‌ی واگرایی از  $20$  تا  $2/5$  درجه و عدد هارتمن از صفر تا  $8$  تغییر می‌کند، مقدار عدد رینولدز نقطه‌ی جدایش از  $52/94$  به  $1862/78$  افزایش یافته که سبب تاخیر در جدایش لایه‌ی مرزی می‌شود. علاوه بر این، از دیدگاه فیزیکی نیز تأثیر شدت میدان مغناطیسی بر جدایش لایه‌ی مرزی بررسی شده است. همچنین، مشاهده می‌شود که با افزایش شدت میدان مغناطیسی، تنش برشی روی دیوار افزایش می‌یابد که منجر به تاخیر در جدایش لایه‌ی مرزی می‌شود.

---